Received: 24 October 2022 | Revised: 28 January 2023 | Accepted: 31 January 2023

DOI: 10.1111/mpp.13311

Molecular Plant Pathology WILEY

ORIGINAL ARTICLE

Tomato chlorosis virus p22 interacts with NbBAG5 to inhibit autophagy and regulate virus infection

Kaijie Shang[1,2] | Li Xiao[1] | Xianping Zhang[1] | Lianyi Zang[1] | Dan Zhao[1] | Chenchen Wang[2] | Xipan Wang[2] | Tao Zhou[3] | Changxiang Zhu[2] | Xiaoping Zhu[1]

[1]College of Plant Protection, Shandong Agricultural University, Tai'an, China

[2]State Key Laboratory of Crop Biology, College of Life Sciences, Shandong Agricultural University, Tai'an, China

[3]State Key Laboratory for Agro-Biotechnology, and Ministry of Agriculture and Rural Affairs, Key Laboratory for Pest Monitoring and Green Management, Department of Plant Pathology, China Agricultural University, Beijing, China

Correspondence
Changxiang Zhu, State Key Laboratory of Crop Biology, College of Life Sciences, Shandong Agricultural University, Tai'an, Shandong 271018, China.
Email: zhchx@sdau.edu.cn

Xiaoping Zhu, College of Plant Protection, Shandong Agricultural University, Tai'an, Shandong 271018, China.
Email: zhuxp@sdau.edu.cn

Funding information
Key R&D Program of Shandong Province, Grant/Award Number: 2022CXGC020710; National Natural Science Foundation of China, Grant/Award Number: 31720103912; Shandong "Double Tops" Program, Grant/Award Number: SYL2017XTTD11; Shandong Provincial Agricultural Major Applied Technology Innovation Project, Grant/Award Number: SD2019ZZ004

Abstract

Tomato chlorosis virus (ToCV) is a member of the genus *Crinivirus* in the family *Closteroviridae*. It has a wide host range and wide distribution, causing serious harm to the vegetable industry. The autophagy pathway plays an important role in plant resistance to virus infection. Viruses and plant hosts coevolve in defence and antidefence processes around autophagy. In this study, the interaction between ToCV p22 and *Nicotiana benthamiana* B-cell lymphoma2-associated athanogenes5 *Nicotiana benthamiana* (NbBAG5) was examined. Through overexpression and down-regulation of NbBAG5, results showed that NbBAG5 could negatively regulate ToCV infection. NbBAG5 was found to be localized in mitochondria and can change the original localization of ToCV p22, which is colocalized in mitochondria. NbBAG5 inhibited the expression of mitophagy-related genes and the number of autophagosomes, thereby regulating viral infection by affecting mitophagy. In summary, this study demonstrated that ToCV p22 affects autophagy by interacting with NbBAG5, established the association between viral infection, BAG proteins family, and the autophagy pathway, and explained the molecular mechanism by which ToCV p22 interacts with NbBAG5 to inhibit autophagy to regulate viral infection.

KEYWORDS
autophagy, B-cell lymphoma2 associated athanogenes, tomato, tomato chlorosis virus, viral infection

1 | INTRODUCTION

The direct losses caused by plant viruses worldwide each year amount to tens of billions of dollars (Godfray et al., 2010). The interaction between virus and host proteins is the key to determine whether the virus can invade the host and effectively replicate and spread in the host (Pallas & García, 2011; Rothenburg & Brennan, 2020). Studies on the molecular mechanism of the interaction between virus and host plant are crucial for clarifying the process of virus infecting plants and finding efficient antiviral strategies.

Kaijie Shang, Li Xiao, and Xianping Zhang contributed equally.

The process in which cells transport denatured proteins, oxidized lipids, and damaged and senescent organelles to lysosomes or vacuoles for digestion and degradation is autophagy, whereas the process of mitochondrial degradation that clears dysfunctional or redundant mitochondria and maintains mitochondrial balance in cells is mitophagy (Alers et al., 2012; Ng et al., 2014; Van Aken & Van Breusegem, 2015). In *Arabidopsis*, autophagy-related protein 1 (ATG1) and ATG13 can form an ATG1-ATG13 kinase complex, which can initiate autophagy by linking metabolic and environmental signals to autophagic vesicles through changes in the phosphorylation status of ATG1 and ATG13 (Mizushima, 2010; Suttangkakul et al., 2011). AtATG11 can be used as the main structural scaffold to connect the ATG1-ATG13 kinase complex with the autophagic mitochondria and autophagosome membrane to participate in the selective autophagy of mitochondria (Li & Vierstra, 2014). ATG1, ATG11, and membrane receptor-like proteins bind to ATG8-phosphatidylethanolamine-modified autophagic vesicles to form autophagosomes, triggering mitochondrial degradation (Broda et al., 2018; Li et al., 2014). In addition, mitochondrial outer membrane protein hexokinase 1, translocases TOM20-2, TOM20-3, TOM20-4, and mitochondrial calcium uniporter proteins MCU1, MCU6 have been found to be associated with mitochondrial autophagy (Broda et al., 2018; Duncan et al., 2011; Teardo et al., 2017).

Virus infection triggers autophagy in host cells to form autophagic vacuoles to engulf the virus and transport it to lysosomes for degradation, but, correspondingly, many viruses can successfully evade host autophagy degradation and even use autophagy for self-replication (Clavel et al., 2017; Levine et al., 2011; Yang et al., 2020). After hepatitis C virus infects the host, it can stimulate the autophagic response of host cells and use the autophagic membrane to replicate the virus and assemble and release virus particles (Ke & Chen, 2014). The unassembled capsid protein of cauliflower mosaic virus (CaMV) can be recognized by the host and degraded by selective autophagy, limiting virus replication (Hafrén et al., 2017). The key autophagy protein ATG8 in the plant autophagy pathway interacts with the virulence factor Bc1 of cotton leaf curl magnolia virus to inhibit virus infection (Haxim et al., 2017). The silencing suppressor HcPro of turnip mosaic virus can inhibit host cell autophagy and promote virus infection (Hafrén et al., 2018). The γb protein of barley stripe mosaic virus disrupts the autophagy pathway by disrupting the ATG7-ATG8 interaction to promote viral infection (Yang et al., 2018). Autophagy resists cucumber mosaic virus infection by degrading the viral 2b protein (Shukla et al., 2022). Chinese wheat mosaic virus negatively regulates plant autophagy and promotes virus infection by interacting with cytosolic glyceraldehyde-3-phosphate dehydrogenase of host cells (Niu et al., 2022). Research on plant viruses and hosts around mitophagy is still in its infancy.

B-cell lymphoma2-associated athanogenes (BAGs) are a family of evolutionarily conserved proteins that are widely present in higher plants and are mainly involved in plant growth and stress response. BAG protein can interact with B-cell lymphoma 2 (Bcl-2) protein to enhance the anti-apoptotic effect of Bcl-2 and increase cell viability (Takayama et al., 1995). AtBAG5 can interact with calmodulin CaM and heat shock protein Hsc70 to form a signal complex, which dynamically regulates the senescence process of leaves (Li, Xing, et al., 2016). *Arabidopsis* AtBAG7 is located on the endoplasmic reticulum and is translocated to the nucleus under heat stress, resulting in heat tolerance (Li et al., 2017). In a study of plant disease resistance, transgenic banana plants overexpressing MusaBAG1 increased resistance to banana wilt (Ghag et al., 2014). AtBAG6 can be cleaved under the regulation of aspartyl protease (APCB1). When infected by *Botrytis cinerea*, the cleaved AtBAG6 regulates the defence response of plants to pathogen infection by inducing the autophagy of plant cells (Li, Kabbage, et al., 2016). Rice OsBAG4 can interact with E3 ubiquitin ligase and participate in rice immune regulation (You et al., 2016). However, little is known about the role of BAG proteins in viral infections.

In 1998, tomato chlorosis virus (ToCV), which can cause the yellowing of tomato leaves, was first discovered in Florida (Wisler et al., 1998). It has now been widely spread worldwide, causing serious losses to the vegetable industry (Fiallo-Olivé et al., 2011; Fiallo-Olivé & Navas-Castillo, 2019; Martínez-Zubiaur et al., 2008). Studies have shown that the p22 protein encoded by ToCV has strong RNA silencing inhibitory activity and preferentially binds to long double-stranded (ds) RNA to inhibit the production of small RNA (Cañizares et al., 2008; Landeo-Ríos et al., 2016b). A p22-deficient ToCV mutant reduced virus accumulation after infection of *Nicotiana benthamiana* (Landeo-Ríos et al., 2016a). The heterologous expression of p22 in plants aggravates the symptoms of plants after infection, leading to plant death (Cañizares et al., 2008; Landeo-Ríos et al., 2017). These reports indicate that p22 plays an important role in ToCV infection. A recent study found that ToCV p22 can interact with S-phase kinase-associated protein 1 (SKP1) of *N. benthamiana* and interfere with the assembly of the SCF^{TIR1} complex (SKP1-Cullin-F-box) by binding to the C-terminus of SKP1, destroying the stability of SCF^{TIR1}; as a result, auxin signal transduction is inhibited, thereby enhancing viral infection (Liu et al., 2021). However, the relationship between ToCV infection and autophagy has not been reported.

This study verified the interaction between ToCV p22 and BAG family proteins in *N. benthamiana* and found that NbBAG5 can negatively regulate ToCV infection in *N. benthamiana*. In addition, NbBAG5 was localized in mitochondria and regulated the expression of mitophagy-related genes, thereby regulating virus infection by affecting mitophagy.

2 | RESULTS

2.1 | Screening of interaction proteins of ToCV p22

ToCV p22 protein is a multifunctional viral protein that plays a key role in promoting viral infection (Cañizares et al., 2008; Landeo-Ríos et al., 2016b; Liu et al., 2021). To study further the mechanism of ToCV p22 protein in virus infection, we constructed the BD-p22 recombinant plasmid for tomato nuclear yeast library screening and found that ToCV p22 could interact with tomato

protein SlBAG4. The interaction was further verified by cotransfection of recombinant plasmids BD-p22 and AD-SlBAG4 into yeast (Figure 1a). We cloned eight homologous NbBAG genes according to the existing sequences in the NCBI database, namely, NbBAG1 to NbBAG8 (Figure S1a,b). The recombinant plasmids BD-p22 and AD-NbBAG1–8 were cotransformed into yeast, respectively. The results showed that ToCV p22 interacted with NbBAG3, NbBAG4, and NbBAG5 in yeast (Figure 1b,c).

2.2 | ToCV p22 interacts with NbBAG5

We selected NbBAG5 (GenBank accession no. XM_016633002) for interaction verification with ToCV and began further research. ToCV p22 and NbBAG5 were connected to the N-terminus and C-terminus of the yellow fluorescent protein YFP, respectively, and transformed into *Agrobacterium tumefaciens*. The *Agrobacterium* solution with different fluorescent protein ends was combined in pairs to infiltrate the leaves of *N. benthamiana*. After 3 days of inoculation, the *N. benthamiana* leaf cells were observed by laser confocal microscopy. The results showed that the yellow fluorescence of the two inoculation combinations of p22 and NbBAG5 was distributed in the cytoplasm and formed some dot-like particles in the cells. The yellow fluorescence signal could not be observed in the negative control group (Figure 2a). Furthermore, ToCV p22 could interact with NbBAG5 in plants by bimolecular fluorescence complementation assay.

To verify further the interaction between ToCV p22 and NbBAG5 in plants, p22-3FLAG and NbBAG5-3Myc recombinant plasmids were constructed in this experiment. The combination of p22-3FLAG and GUS-3Myc was used as a negative control, and *Agrobacterium* infiltration was used to inoculate the *N. benthamiana* leaves. Three days later, the inoculated leaves were collected to extract the total plant protein. Western blot analysis showed that all the proteins were expressed normally in the leaves (Figure 2b). Co-immunoprecipitation of the extracted total protein with anti-FLAG antibody magnetic beads revealed that ToCV p22 could interact with NbBAG5 in plants (Figure 2b).

In accordance with the prediction results of NbBAG5's secondary structure, tertiary structure, and main domain (Figure S1c), the following deletion mutants of NbBAG5 were constructed: AD-NbBAG5Δ1 (1–48 amino acids), AD-NbBAG5Δ2 (49–156 amino acids), and AD-NbBAG5Δ3 (157–203 amino acids). Yeast two-hybrid experiments showed that only the combination of AD-NbBAG5Δ2 + BD-p22 could make yeast grow normally on SD/−Leu/−Trp/−His/−Ade quadruple dropout medium (Figure 2c). This deletion mutant contains the BAG domain, indicating that the BAG domain (74–151 amino acids) is a key functional domain for the interaction between NbBAG5 and ToCV p22.

2.3 | NbBAG5 negatively regulates ToCV infection

To study further the effect of NbBAG5 on ToCV infection, we used the *Agrobacterium* infiltration method to inoculate ToCV infectious clones on *N. benthamiana*. After 28 days, the symptoms of *N. benthamiana* were observed. Compared with healthy plants, diseased plants

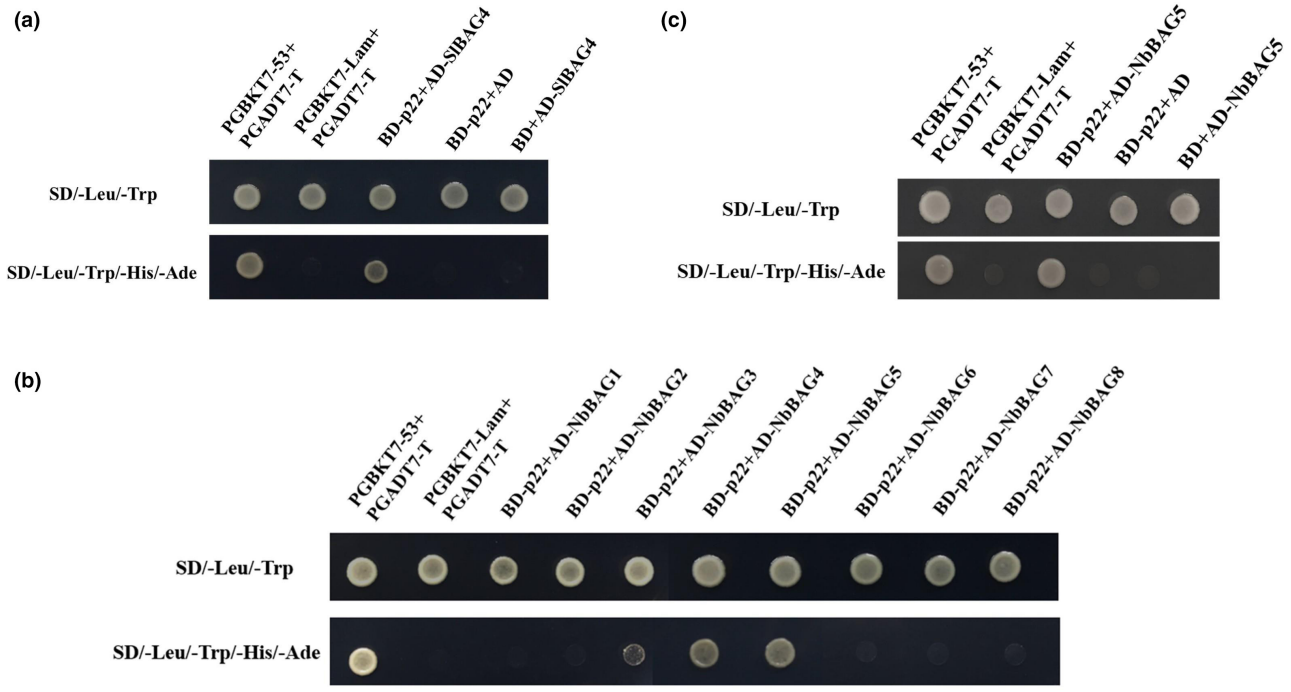

FIGURE 1 Screening of interaction proteins of ToCV p22. (a) The interaction between ToCV p22 and SlBAG4 was verified by yeast two-hybrid assay. (b) The NbBAG proteins interacting with ToCV p22 were screened by yeast two-hybrid assay. (c) The interaction between ToCV p22 and NbBAG5 was verified by yeast two-hybrid assay.

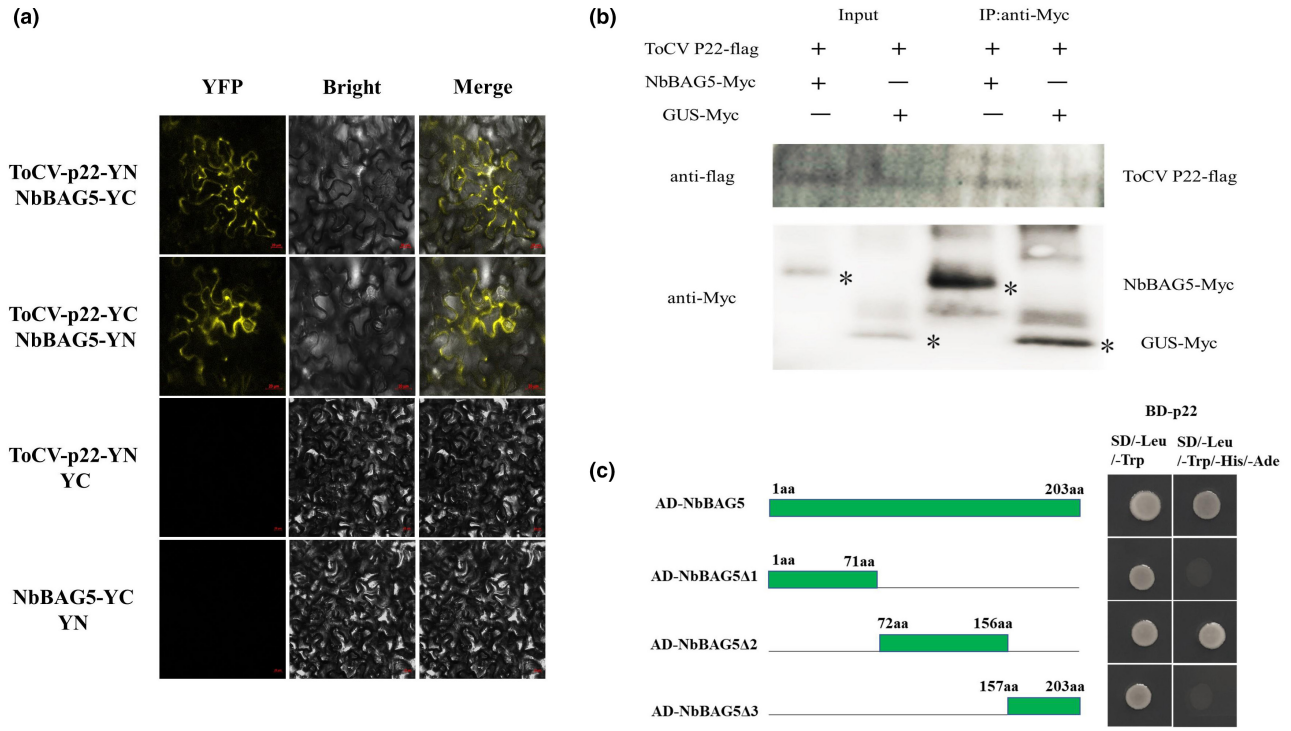

FIGURE 2 ToCV p22 interacts with NbBAG5. (a) The interaction between ToCV p22 and NbBAG5 was verified by bimolecular fluorescence complementation assay. From left to right, yellow fluorescent protein (YFP), bright-field of vision, combined fields of vision, scale 20 μm. YN and YC are empty vector controls. (b) The interaction between ToCV p22 and NbBAG5 was verified by co-immunoprecipitation experiments. The asterisks indicate the position of the target band. (c) The interaction domain of NbBAG5 and ToCV p22 was verified by yeast two-hybrid assay.

showed chlorotic and yellow spot symptoms (Figure S2a). Total RNA was extracted from the upper leaves for reverse transcription (RT)-PCR detection (Figure S2b). The changes of *NbBAG5* gene content after ToCV infection were examined by RT-quantitative PCR (RT-qPCR). The results showed that the content of *NbBAG5* gene in ToCV-infected plants increased to 2.12 times compared with healthy plants (Figure S2c). ToCV infection can promote the up-regulation of *NbBAG5* gene expression. We found that the content of *NbBAG5* gene in *N. benthamiana* stably overexpressing ToCV p22 was 1.71 times that of wild-type *N. benthamiana* by RT-qPCR (Figure S2d). Stable overexpression of ToCV p22 can also promote the up-regulation of *NbBAG5* gene expression.

The *NbBAG5* gene sequence was silenced by TRV-*NbBAG5*, and the symptoms were observed after 8 days of inoculation. The leaves of TRV-*PDS* (*phytoene desaturase*)-inoculated plants were albino, and TRV-*NbBAG5*-inoculated plants had no significant phenotypic changes compared with TRV-*GUS* (*β-glucuronidase*) (Figure 3a). RT-qPCR showed that the content of the *NbBAG5* gene in TRV-*NbBAG5* inoculated plants was 0.57 times that of normal plants (Figure 3b). ToCV infectious clones were inoculated in *NbBAG5*-silenced *N. benthamiana* (Figure 3c). After 28 days, total RNA was extracted from the upper leaves. RT-qPCR showed that the accumulation of ToCV coat protein (CP) in *NbBAG5*-silenced *N. benthamiana* plants was 2.72 times that of nonsilenced *NbBAG5* plants (Figure 3d). The results showed that the gene silencing of *NbBAG5* could increase the virus accumulation and promote the infection of ToCV.

To clarify the effect of *NbBAG5* gene expression level on ToCV infection, the PVX vector pGR106 was used for a gene overexpression test. The constructed recombinant plasmid pGR106-*NbBAG5* was transferred into *Agrobacterium* and a pGR106 empty vector was used as control to infiltrate *N. benthamiana* leaves. The symptoms were observed 8 days after inoculation. The plants inoculated with pGR106 showed mosaic symptoms and the plants inoculated with pGR106-*NbBAG5* showed lighter symptoms (Figure 3e). RT-qPCR showed that the gene content of *NbBAG5* in *N. benthamiana* plants inoculated with pGR106-*NbBAG5* was 6.09 times that of the control treatment (Figure 3f). ToCV infectious clones were inoculated in *N. benthamiana* plants overexpressing *NbBAG5* (Figure 3g). After 28 days, the upper leaves were collected for RT-qPCR to examine the change of ToCV CP systemic accumulation. The results showed that the ToCV CP accumulation of pGR106-NbBAG5 treatments plants was down-regulated to 0.47 times that of the control plants (Figure 3h). The results showed that overexpression of *NbBAG5* gene could reduce virus accumulation after ToCV infection and overexpression of *NbBAG5* could inhibit the infection of ToCV.

2.4 | NbBAG5 and ToCV p22 colocalized in mitochondria

The diversity of BAG protein structure leads to different subcellular localizations, which is closely related to its function (Doukhanina

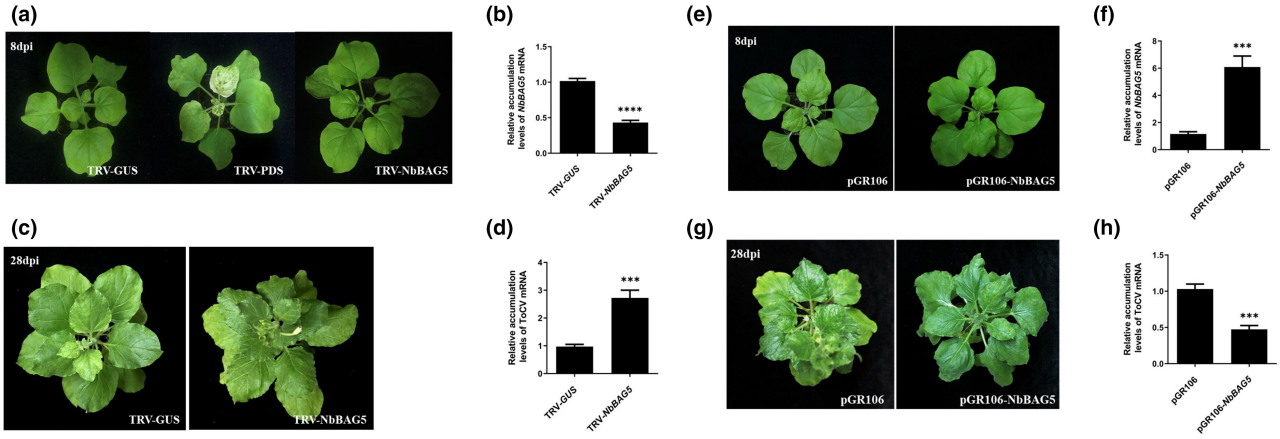

FIGURE 3 NbBAG5 negatively regulates ToCV infection. (a) Phenotype of *Nicotiana benthamiana* after 8 days of *Agrobacterium* infection containing TRV modified vector. (b) The down-regulation of *NbBAG5* in *N. benthamiana* was detected by reverse transcription-quantitative PCR (RT-qPCR) detection. (c) Phenotype of ToCV 28 days after inoculation on *N. benthamiana* infected with *Agrobacterium* containing TRV modified vector. (d) RT-qPCR detection of ToCV accumulation in *N. benthamiana*. (e) Phenotype of *N. benthamiana* 8 days after infection with *Agrobacterium* containing pGR106 modified vector. (f) RT-qPCR detection of *NbBAG5* overexpression in *N. benthamiana*. (g) Phenotype of ToCV 28 days after inoculation on *N. benthamiana* infected with *Agrobacterium* containing pGR106 modified vector. (h) RT-qPCR detection of ToCV accumulation in *N. benthamiana*. Data were collected in three biological experiments, and the bar value represents the standard deviation. The statistical analysis was based on Student's *t* test, $^{***}p < 0.001$, $^{****}p < 0.0001$.

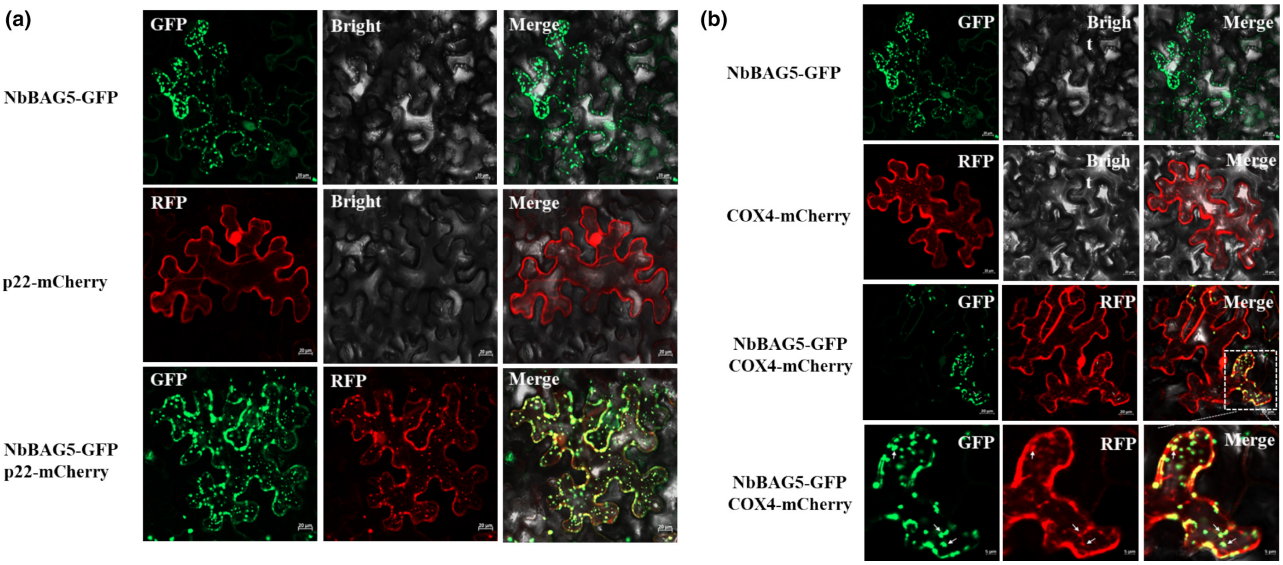

FIGURE 4 NbBAG5 and ToCV p22 colocalized in mitochondria. (a) Subcellular colocalization of NbBAG5 and ToCV p22 was observed by laser confocal microscopy. (b) Subcellular colocalization of NbBAG5 and COX4 was observed by laser confocal microscopy. The scale is 20 μm and the enlarged scale is 5 μm.

et al., 2006; Kabbage et al., 2016; Kabbage & Dickman, 2008). To explore the localization of NbBAG5 in plant cells, the NbBAG5-GFP (green fluorescent protein) recombinant plasmid was constructed in this experiment. The NbBAG5-GFP recombinant plasmid was infiltrated into *N. benthamiana* leaves by *Agrobacterium* alone or co-infiltration with p22-mCherry. After 3 days, the fluorescent protein signal in leaf cells was observed by laser confocal microscopy. The results showed that NbBAG5 had special localization and formed many punctate particles in cells. The colocalization of NbBAG5 and p22 could change the subcellular localization of p22. The red fluorescent protein signal of p22 alone was only distributed in the cytoplasm and nucleus. After colocalization with NbBAG5, some punctate particles were also formed in cells, indicating that NbBAG5 interacted with p22 in plant cells and changed the subcellular localization of p22 (Figure 4a).

NbBAG5 was predicted to be a plant mitochondrial localization protein. To verify the special localization of NbBAG5, a mitochondrial localization marker COX4-mCherry was constructed. By laser confocal microscopy, NbBAG5 colocalized with the mitochondrial localization marker in mitochondria and NbBAG5 was identified as

a mitochondrial localization protein (Figure 4b). In combination with the colocalization results of NbBAG5 and p22, the results showed that NbBAG5 could change the subcellular localization of p22 by interaction, so that p22 was also localized in mitochondria.

2.5 | NbBAG5 inhibits autophagy induced by ToCV infection

The autophagy pathway is the focus of defence and antidefence between host and virus (Clavel et al., 2017; Dong & Levine, 2013; Yang et al., 2020). According to the localization of NbBAG5, we used pGR106-NbBAG5 and virus-induced gene silencing of *NbBAG5* treatments *N. benthamiana* plants to detect the expression level of mitochondrial autophagy-related genes by RT-qPCR. The results showed that compared with the control, the mitophagy-related genes *ATG1*, *ATG8*, *ATG11*, *ATG13*, and *MCU6* in *NbBAG5* gene-silenced plants were up-regulated to 1.67, 2.16, 2.03, 1.46, and 1.63 times, respectively, and *Hxk1* had no significant change (Figure 5a). The mitophagy-related genes *ATG1*, *ATG8*, *ATG11*, *ATG13*, and *MCU6* in *NbBAG5*-overexpressing plants were down-regulated to 0.75, 0.76, 0.64, 0.48, and 0.47 times, respectively, and *Hxk1* did not change significantly (Figure 5b). These results indicate that NbBAG5 can regulate the expression level of mitophagy-related genes.

We extracted RNA from ToCV-infected and stably overexpressing ToCV p22 protein *N. benthamiana* for RT-qPCR. Compared with the control, the results showed that the expression levels of *ATG1*, *ATG11*, *ATG13*, and *Hxk1* in *N. benthamiana* stably overexpressing ToCV p22 protein did not change significantly, while the expression levels of *ATG8* and *MCU6* increased by 1.15 and 4.74 times (Figure 5c). The expression levels of *ATG1*, *ATG8*, *ATG11*, *ATG13*, and *MCU6* increased by 2.83, 3.01, 2.54, 2.59, 6.09, and 2.67 times in ToCV-infected *N. benthamiana* (Figure 5d). This indicates that the level of autophagy increased slightly when ToCV p22 protein was stably overexpressed, while ToCV infection activated autophagy. We transiently overexpressed *NbBAG5* in ToCV-infected *N. benthamiana* and performed RT-qPCR after 3 days. The results showed that the expression levels of *ATG1*, *ATG8*, *ATG11*, *ATG13*, *Hxk1*, and *MCU6* were down-regulated to 0.59, 0.59, 0.66, 0.81, 0.31, and 0.40 times in comparison with ToCV-infected *N. benthamiana*, indicating that NbBAG5 can inhibit ToCV infection-induced autophagy (Figure 5e).

We constructed the pCa-ATG8-CFP (cyan fluorescent protein) expression vector and carried out *Agrobacterium* infection of stable overexpression of ToCV p22 and ToCV-infected *N. benthamiana*. After 3 days, the number of autophagosomes was observed by laser confocal microscopy. The results showed that the accumulation of autophagosomes in tobacco leaves overexpression of ToCV p22 and infected with ToCV was more than that of wild-type

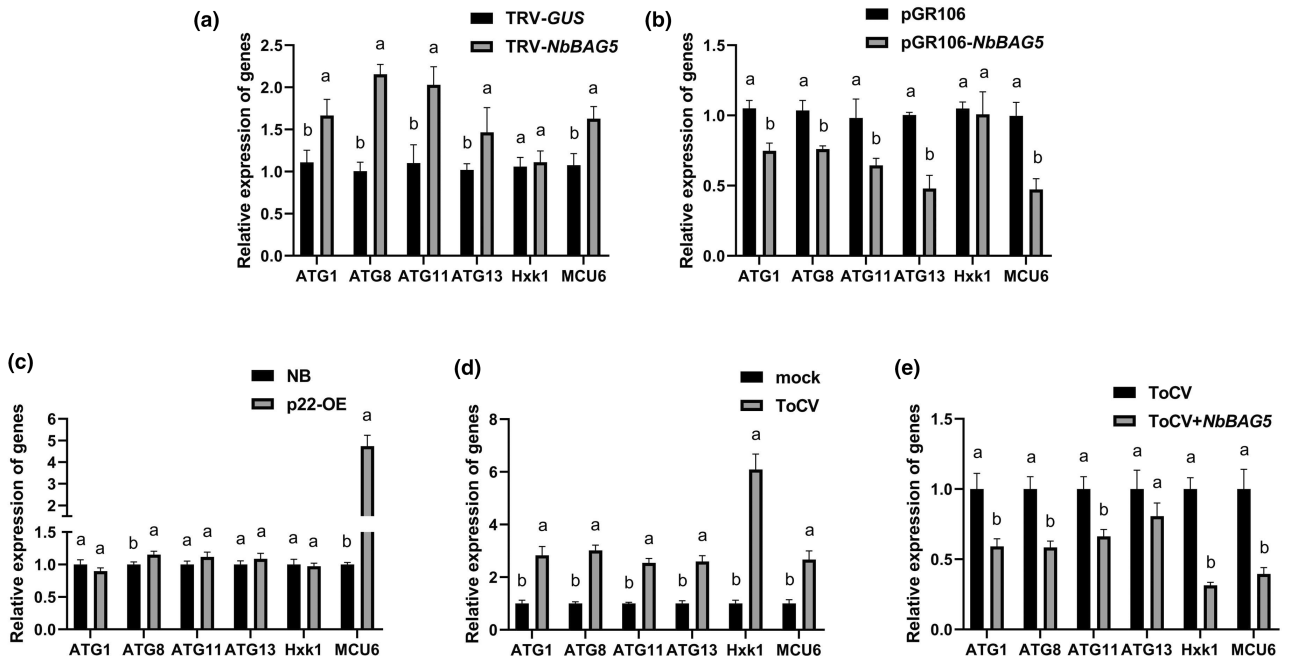

FIGURE 5 Effect of NbBAG5 on gene expression of autophagy pathway. (a) The effect of down-regulation of *NbBAG5* on the expression of autophagy pathway genes was detected by reverse transcription-quantitative PCR (RT-qPCR) in *Nicotiana benthamiana*. (b) The effect of the overexpression of *NbBAG5* on the expression of autophagy pathway genes was detected by RT-qPCR in *N. benthamiana*. (c) The effect of the overexpression of ToCV p22 on the expression of autophagy pathway genes was detected by RT-qPCR in *N. benthamiana*. (d) The effect of ToCV infection on the expression of autophagy pathway genes was detected by RT-qPCR in *N. benthamiana*. (e) The effect of the overexpression of *NbBAG5* on the expression of autophagy pathway genes in ToCV-infected *N. benthamiana* was detected by RT-qPCR. Data were collected in three biological experiments and the bar value represents the standard deviation. The statistical analysis was based on Student's *t* test. The difference between a and b indicates a significant difference of at least $p < 0.05$.

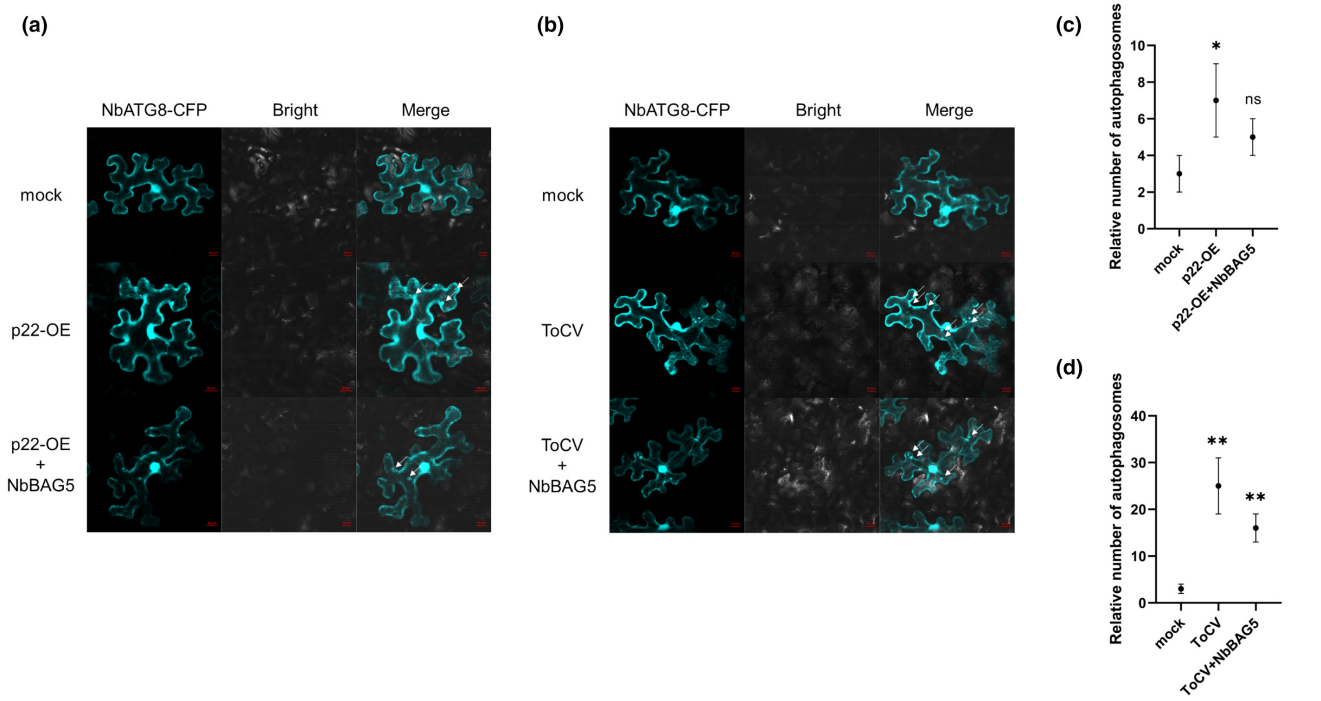

FIGURE 6 NbBAG5 inhibits autophagy induced by ToCV infection. (a) The effect of transient expression of *NbBAG5* on the number of autophagosomes in stable overexpression ToCV p22 *Nicotiana benthamiana* was observed by laser confocal microscopy. (b) The effect of transient expression of *NbBAG5* on the number of autophagosomes in ToCV-infected *N. benthamiana* was observed by laser confocal microscopy. (c) Comparison and statistics of the relative number of autophagosomes in (a). (d) Comparison and statistics of the relative number of autophagosomes in (b). The scale is 50 μm. Data were collected in three biological experiments and the bar value represents the standard deviation. The statistical analysis was based on Student's *t* test. ns, not significant. $^{*}p < 0.05$, $^{**}p < 0.01$.

N. benthamiana (Figure 6a,b). *NbBAG5* and *ATG8-CFP* were transiently overexpressed in *N. benthamiana* stably overexpressing ToCV p22. After 3 days, the number of autophagosomes was observed by laser confocal microscopy. The results showed that transient overexpression of *NbBAG5* inhibited the accumulation of autophagosomes in *N. benthamiana* leaves stably overexpressing ToCV p22 (Figure 6a,c). *NbBAG5* and *ATG8-CFP* were transiently overexpressed in ToCV-infected *N. benthamiana*. After 3 days, the number of autophagosomes was observed by laser confocal microscopy. It was found that NbBAG5 transient overexpression inhibited the accumulation of autophagosomes in ToCV-infected *N. benthamiana* leaves (Figure 6b,d). The above results indicate that ToCV infection activates autophagy and NbBAG5 can inhibit ToCV infection-induced autophagy to regulate viral infection.

3 | DISCUSSION

In this study, we verified the interaction between ToCV p22 and NbBAG5. The *NbBAG5* gene was up-regulated in ToCV-infected *N. benthamiana* plants and played a negative regulatory role in the process of ToCV infection. Subcellular colocalization observation showed that NbBAG5 was a mitochondrial localization protein. The interaction between ToCV p22 and NbBAG5 can change the localization of ToCV p22, so that the fluorescence signal of ToCV p22 is distributed in mitochondria, indicating that the final stable interaction site between ToCV p22 and NbBAG5 is mitochondria, and the response of NbBAG5 to ToCV infection may also be conducted in mitochondria. RT-qPCR and autophagosome observation revealed that NbBAG5 inhibited ToCV infection-induced autophagy, therefore ToCV p22 protein interacted with NbBAG5 to regulate autophagy to promote virus infection.

Autophagy plays an important role in the process of plant resistance to virus invasion. Many viruses have also evolved mechanisms to evade or utilize host autophagy degradation, which promotes the coevolution of hosts and viruses (Deretic & Levine, 2009; Dreux & Chisari, 2010; Mizushima et al., 2008). During tobacco mosaic virus infection in tomato, autophagy is activated and responsible for scavenging reactive oxygen species, maintaining the coexistence of virus and host cells (Zhou et al., 2018). To counteract remorin-mediated host response, rice stripe virus-encoded NSvc4 protein can interfere with the S-acylation of remorin and induce its degradation via autophagy (Fu et al., 2018). Cotton leaf curl multan virus bC1 induces autophagy by disrupting the interaction of ATG3 with glyceraldehyde-3-phosphate dehydrogenases (Ismayil et al., 2020). *N. benthamiana* P3IP protein interacts with rice stripe virus p3 protein and mediates its autophagic degradation to limit viral infection (Jiang et al., 2021). The best way for virus and host to coexist is long-term parasitic coexistence, and the regulation of host resistance response is an important part of

long-term parasitic virus. Our study provides a basis for the study of the defence and antidefence competition between plant hosts and viruses around autophagy.

The p22 protein encoded by ToCV RNA1 is a silencing suppressor and plays an important role in viral infection. ToCV p22 can effectively inhibit the local RNA silencing induced by sense-strand RNA or double-stranded RNA and regulate the balance between the sense and antisense strands of the virus during viral infection (Cañizares et al., 2008; Landeo-Ríos et al., 2016b). Research on ToCV p22 is mostly on its silencing activity, and a few studies focus on its pathogenic mechanism and interaction mechanism with host proteins. A recent study showed that p22 could interact with S-phase kinase-associated protein 1 (SKP1) of *N. benthamiana*, disrupt auxin signal transduction, and promote ToCV infection (Liu et al., 2021). We found that ToCV p22 can activate autophagy, but stable overexpression of ToCV p22 activates autophagy less than ToCV infection. This may be because the autophagy pathway in *N. benthamiana* stably overexpressing ToCV p22 has reached a relatively balanced state, which also suggests that there may be other mechanisms to activate autophagy during ToCV infection. Interestingly, only a part of ToCV p22 changed its original localization by interacting with NbBAG5. There should be other host proteins that also have other colocalization with ToCV p22, which also indicates that ToCV p22 has more biological functions.

BAG family proteins have various biological functions. Studies have shown that they play an important role in plant growth and development, and stress resistance (Doukhanina et al., 2006; Li et al., 2017). In terms of plant disease resistance, transgenic banana plants overexpressing MusaBAG1 increase resistance to banana Fusarium wilt (Ghag et al., 2014). AtBAG6 regulates the defence response of *Arabidopsis* to *B. cinerea* infection (Li, Kabbage, et al., 2016). OsBAG4 is involved in rice disease resistance by interacting with E3 ubiquitin ligase (You et al., 2016). We found that NbBAG5 changed the original localization of some ToCV p22 by interaction, and finally colocalized in mitochondria and affected mitophagy. The specific process of NbBAG5 affecting the autophagy pathway should be the focus of subsequent research.

The interaction of viral pathogenicity factors and host factors affects viral pathogenicity, which is a hot topic in viral molecular biology. We found that ToCV p22 can interact with NbBAG5, and NbBAG5 inhibits ToCV infection in *N. benthamiana*. Further study found that NbBAG5 is located in mitochondria, NbBAG5 can change the subcellular localization of ToCV p22 by interaction, and hijacking p22 is also located in mitochondria. Silencing NbBAG5 can up-regulate the expression of mitophagy-related genes, and overexpression of NbBAG5 can down-regulate the expression of mitophagy-related genes. NbBAG5 could inhibit autophagy induced by ToCV infection in *N. benthamiana*. Our study established the association between viral infection, BAG family proteins, and the autophagy pathway, thus contributing to the understanding of the interaction between viral proteins and host proteins to regulate their own infection and the production value in molecular breeding antiviral work.

4 | EXPERIMENTAL PROCEDURES

4.1 | Plant materials and growth condition

The seeds of *N. benthamiana* used in this study were preserved by Shandong Agricultural University in Tai'an, China. The seeds were germinated on MS solid medium and planted in a small pot with nutrient soil in the culture room. It was grown in a culture chamber with a relative humidity of 65%, a light time of 16 h (25°C) and a dark time of 8 h (20°C).

4.2 | *Agrobacterium* infiltration and virus inoculation

In accordance with the method of our laboratory (Shang et al., 2022), the *Agrobacterium* was suspended in solution (10 mM $MgCl_2$, 10 mM MES [pH 5.6], 100 μM acetosyringone) and the OD_{600} of each culture was adjusted to 0.5 before infiltration. A needleless syringe was used to penetrate the paraxial side of the 4-week-old *N. benthamina* leaves. Each experiment was repeated independently three times.

The recombinant plasmids of tobacco rattle virus (TRV), pGR106 (potato virus X, PVX) virus and ToCV infectious clone pCass4-Rz-ToCV were preserved in our laboratory (Liu et al., 2021). The recombinant plasmids of TRV-NbBAG5 and pGR106-NbBAG5 were obtained by inserting the *NbBAG5* gene between the CaMV 35S promoter and the Nos terminator of the TRV recombinant plasmid and the pGR106 virus recombinant plasmid, respectively (Figure S3). The infiltrated leaves were collected for RNA extraction and RT-qPCR detection after 3 days of infiltration. *Escherichia coli* DH5α was used to propagate and purify plasmids.

4.3 | Sequence analysis

The NbBAG5 (XM_016633002) sequence was derived from the National Center for Biotechnology Information (NCBI). Protein domain prediction was performed using the SMART online analysis site (http://smart.embl-heidelberg.de/). A phylogenetic tree was constructed by MEGA 7 software and neighbour-joining method (number of bootstrap replications 1000, p-distance selected in model/method, and complete deletion selected in gaps/missing data treatment). The tertiary structure of protein was analysed by the online software Swiss-model (https://swissmodel.expasy.org/) using the default parameters of automatic modelling.

4.4 | Yeast two-hybrid assay and yeast library screening

NbBAG1-8 and ToCV p22 were ligated between the T7 promoter and Nos terminator of pGADT7 plasmid and pGBKT7 plasmid, respectively. The yeast expression plasmids of pGADT7-NbBAG1-8

and pGBKT7-ToCV p22 were obtained. In reference to the yeast two-hybrid method (Liu et al., 2021), the recombinant plasmids pGADT7-NbBAG1-8 and pGBKT7-ToCV p22 were cotransformed into yeast and plated on SD/−Leu/−Trp double-dropout (DDO) medium and SD/−Leu/−Trp/−His/−Ade quadruple dropout (QDO) medium, respectively, and were observed after 3 days of inverted culture in an incubator at 30°C. BD-ToCV p22 was used as the bait protein to screen the tomato nuclear yeast library. The activated library liquid was first spread on the DDO medium, and then the monoclonal yeast was picked and streaked on the QDO medium. ADT7 primer and AD3R primer were used to clone the gene after 3 days of inverted culture in an incubator at 30°C, and the gene sequence of the interaction protein was obtained by sequencing.

4.5 | Bimolecular fluorescence complementation assay

In reference to the method (Niu et al., 2022), ToCV p22 and NbBAG5 were connected to the N-terminus and C-terminus of the yellow fluorescent protein (YFP), respectively. The recombinant plasmid was added to *Agrobacterium* competent cells, frozen in liquid nitrogen for 5 min, in a 37°C water bath for 5 min, with ice cooling for 3 min. The *Agrobacterium* solution with different fluorescent protein ends was combined in pairs to infiltrate the leaves of *N. benthamiana*. After 3 days of infiltration of *N. benthamiana* leaves, a confocal microscope (LSM 880; Zeiss) was used for imaging. YFP was excited at 514 nm and captured at 565–585 nm. Ten independent plants were analysed and the experiment was repeated in three biological replicates.

4.6 | Co-immunoprecipitation assay

In accordance with the method of Liu et al. (2021), p22-3FLAG and BAG5-3Myc recombinant plasmids were constructed using pROKII plasmid as the carrier skeleton. The combination of p22-3FLAG and GUS-3Myc was used as a negative control, and the *Agrobacterium* co-infiltration was used to inoculate the *N. benthamiana* leaves. After 3 days, the total protein of the inoculated leaves was extracted and incubated with anti-FLAG antibody magnetic beads (Sigma-Aldrich) for elution and western blot detection. A 12.5% polyacrylamide gel was used for electrophoresis at a constant voltage of 150 V for 1.5 h and the nitrocellulose membrane was transferred at 400 mA for 1 h. Labelled antibodies were used for hybridization and secondary antibodies were incubated for chemiluminescence detection.

4.7 | RNA extraction and RT-qPCR assay

In accordance with the method of our laboratory (Shang et al., 2022), 0.5 g of infiltrated leaves of *N. benthamiana* was fully ground in a liquid nitrogen mortar, 1 mL of TRIzol (Invitrogen) was added to shake and mix, chloroform was used for extraction, 75% ethanol was used for rinsing after centrifugal separation, and double-distilled water was used for resuspension to obtain an RNA solution. Reverse transcription of cDNA was performed using a reverse transcription kit (Vazyme). qPCR experiments were performed using an SYBR Mix (Vazyme) amplification system in a quantometer (Roche). We used 2 μg of RNA for reverse transcription in each reaction according to the instructions, and the final concentration of qPCR was diluted to 1/20 of the reverse transcription product. The *N. benthamiana actin* gene was used as the internal reference gene. The primers used for the RT-qPCR are listed in Table S1. Data were collected in three biological experiments, and the bar value represents the standard deviation. The statistical analysis was based on Student's *t* test, $^{*}p < 0.05$, $^{**}p < 0.01$, $^{***}p < 0.001$, $^{****}p < 0.0001$.

4.8 | Subcellular colocalization of NbBAG5 and observation of the number of autophagosomes

NbBAG5-GFP, p22-mCherry, and COX4-mCherry recombinant plasmids were constructed using pROKII plasmid as the carrier skeleton (Figure S3). The *Agrobacterium* transformed with NbBAG5-GFP was mixed with the *Agrobacterium* transformed with p22-mCherry and COX4-mCherry to infiltrate *N. benthamiana*. After 3 days of infiltration of *N. benthamiana* leaves, a laser confocal microscope (LSM 880) was used for imaging. GFP was excited at 488 nm and captured at 510–550 nm with a 20× objective lens. Ten independent plants were analysed. The experiment was repeated in three biological replicates.

In reference to the method (Haxim et al., 2017), the NbATG8-CFP recombinant plasmid was constructed and transformed into *Agrobacterium* to infiltrate ToCV-infected *N. benthamiana*, and the *Agrobacterium*-infiltrated normal *N. benthamiana* transformed with NbATG8-CFP recombinant plasmid was used as mock. The ToCV-infected *N. benthamiana* was co-infiltrated with *Agrobacterium* transformed with NbATG8-CFP recombinant plasmid and NbBAG5-GFP recombinant plasmid, and the ToCV-infected *N. benthamiana* was co-infiltrated with *Agrobacterium* transformed with NbATG8-CFP recombinant plasmid as mock. Laser scanning confocal microscopy (LSM 880) was performed 3 days after infiltration of *N. benthamiana* leaves. CFP was excited at 405 nm and captured at 454–581 nm, using a 20× objective lens. Ten independent plants were analysed. The experiment was repeated in three biological replicates.

ACKNOWLEDGEMENTS

This research was funded by the National Natural Science Foundation of China (31720103912), the Shandong Provincial Agricultural Major Applied Technology Innovation Project (SD2019ZZ004), the Key R&D Program of Shandong Province (2022CXGC020710), and the Shandong "Double Tops" Program (SYL2017XTTD11).

CONFLICT OF INTEREST STATEMENT

The authors declare no conflict of interest.

DATA AVAILABILITY STATEMENT

All relevant data and materials that support the findings of this study are available from the corresponding author upon request.

ORCID

Kaijie Shang https://orcid.org/0000-0002-0793-9235
Tao Zhou https://orcid.org/0000-0001-7702-8472
Changxiang Zhu https://orcid.org/0000-0002-5640-6312
Xiaoping Zhu https://orcid.org/0000-0001-7236-731X

REFERENCES

Alers, S., Löffler, A.S., Wesselborg, S. & Stork, B. (2012) Role of AMPK-mTOR-Ulk1/2 in the regulation of autophagy: cross talk, shortcuts, and feedbacks. *Molecular and Cellular Biology*, 32, 2–11.

Broda, M., Millar, A.H. & Van Aken, O. (2018) Mitophagy: a mechanism for plant growth and survival. *Trends in Plant Science*, 23, 434–450.

Cañizares, M.C., Navas-Castillo, J. & Moriones, E. (2008) Multiple suppressors of RNA silencing encoded by both genomic RNAs of the crinivirus, tomato chlorosis virus. *Virology*, 379, 168–174.

Clavel, M., Michaeli, S. & Genschik, P. (2017) Autophagy: a double-edged sword to fight plant viruses. *Trends in Plant Science*, 22, 646–648.

Deretic, V. & Levine, B. (2009) Autophagy, immunity, and microbial adaptations. *Cell Host & Microbe*, 5, 527–549.

Dong, X. & Levine, B. (2013) Autophagy and viruses: adversaries or allies? *Journal of Innate Immunity*, 5, 480–493.

Doukhanina, E.V., Chen, S., Van Der Zalm, E., Godzik, A., Reed, J. & Dickman, M.B. (2006) Identification and functional characterization of the BAG protein family in *Arabidopsis thaliana*. *The Journal of Biological Chemistry*, 281, 18793–18801.

Dreux, M. & Chisari, F.V. (2010) Viruses and the autophagy machinery. *Cell Cycle*, 9, 1295–1307.

Duncan, O., Taylor, N.L., Carrie, C., Eubel, H., Kubiszewski-Jakubiak, S., Zhang, B. et al. (2011) Multiple lines of evidence localize signaling, morphology, and lipid biosynthesis machinery to the mitochondrial outer membrane of *Arabidopsis*. *Plant Physiology*, 157, 1093–1113.

Fiallo-Olivé, E., Hamed, A.A., Moriones, E. & Navas-Castillo, J. (2011) First report of tomato chlorosis virus infecting tomato in Sudan. *Plant Disease*, 95, 1592.

Fiallo-Olivé, E. & Navas-Castillo, J. (2019) Tomato chlorosis virus, an emergent plant virus still expanding its geographical and host ranges. *Molecular Plant Pathology*, 20, 1307–1320.

Fu, S., Xu, Y., Li, C., Li, Y., Wu, J. & Zhou, X. (2018) Rice stripe virus interferes with S-acylation of remorin and induces its autophagic degradation to facilitate virus infection. *Molecular Plant*, 11, 269–287.

Ghag, S.B., Shekhawat, U.K. & Ganapathi, T.R. (2014) Native cell-death genes as candidates for developing wilt resistance in transgenic banana plants. *AoB Plants*, 6, plu037.

Godfray, H.C., Beddington, J.R., Crute, I.R. et al. (2010) Food security: the challenge of feeding 9 billion people. *Science*, 327, 812–818.

Hafrén, A., Macia, J.L., Love, A.J., Milner, J.J., Drucker, M. & Hofius, D. (2017) Selective autophagy limits cauliflower mosaic virus infection by NBR1-mediated targeting of viral capsid protein and particles. *Proceedings of the National Academy of Sciences of the United States of America*, 114, E2026-e35.

Hafrén, A., Üstün, S., Hochmuth, A., Svenning, S., Johansen, T. & Hofius, D. (2018) Turnip mosaic virus counteracts selective autophagy of the viral silencing suppressor HCpro. *Plant Physiology*, 176, 649–662.

Haxim, Y., Ismayil, A., Jia, Q., Wang, Y., Zheng, X., Chen, T. et al. (2017) Autophagy functions as an antiviral mechanism against geminiviruses in plants. *eLife*, 6, e23897.

Ismayil, A., Yang, M., Haxim, Y., Wang, Y., Li, J., Han, L. et al. (2020) Cotton leaf curl Multan virus βC1 protein induces autophagy by disrupting the interaction of autophagy-related protein 3 with glyceraldehyde-3-phosphate dehydrogenases. *The Plant Cell*, 32, 1124–1135.

Jiang, L., Zheng, X., Liu, Y., Chen, J., Lu, Y. & Yan, F. (2021) Plant protein P3IP participates in the regulation of autophagy in *Nicotiana benthamiana*. *Plant Signaling & Behavior*, 16, 1861768.

Kabbage, M. & Dickman, M.B. (2008) The BAG proteins: a ubiquitous family of chaperone regulators. *Cellular and Molecular Life Sciences*, 65, 1390–1402.

Kabbage, M., Kessens, R. & Dickman, M.B. (2016) A plant Bcl-2-associated athanogene is proteolytically activated to confer fungal resistance. *Microbial Cell*, 3, 224–226.

Ke, P.Y. & Chen, S.S. (2014) Autophagy in hepatitis C virus-host interactions: potential roles and therapeutic targets for liver-associated diseases. *World Journal of Gastroenterology*, 20, 5773–5793.

Landeo-Ríos, Y., Navas-Castillo, J., Moriones, E. & Cañizares, M.C. (2016a) The p22 RNA silencing suppressor of the Crinivirus tomato chlorosis virus is dispensable for local viral replication but important for counteracting an antiviral RDR6-mediated response during systemic infection. *Viruses*, 8, 182.

Landeo-Ríos, Y., Navas-Castillo, J., Moriones, E. & Cañizares, M.C. (2016b) The p22 RNA silencing suppressor of the Crinivirus tomato chlorosis virus preferentially binds long dsRNAs preventing them from cleavage. *Virology*, 488, 129–136.

Landeo-Ríos, Y., Navas-Castillo, J., Moriones, E. & Cañizares, M.C. (2017) The heterologous expression of the p22 RNA silencing suppressor of the Crinivirus tomato chlorosis virus from tobacco rattle virus and potato virus X enhances disease severity but does not complement suppressor-defective mutant viruses. *Viruses*, 9, 358.

Levine, B., Mizushima, N. & Virgin, H.W. (2011) Autophagy in immunity and inflammation. *Nature*, 469, 323–335.

Li, F., Chung, T. & Vierstra, R.D. (2014) AUTOPHAGY-RELATED11 plays a critical role in general autophagy- and senescence-induced mitophagy in *Arabidopsis*. *The Plant Cell*, 26, 788–807.

Li, Y., Kabbage, M., Liu, W. & Dickman, M.B. (2016) Aspartyl protease-mediated cleavage of BAG6 is necessary for autophagy and fungal resistance in plants. *The Plant Cell*, 28, 233–247.

Li, F. & Vierstra, R.D. (2014) Arabidopsis ATG11, a scaffold that links the ATG1-ATG13 kinase complex to general autophagy and selective mitophagy. *Autophagy*, 10, 1466–1467.

Li, Y., Williams, B. & Dickman, M. (2017) *Arabidopsis* B-cell lymphoma2 (Bcl-2)-associated athanogene 7 (BAG7)-mediated heat tolerance requires translocation, sumoylation and binding to WRKY29. *The New Phytologist*, 214, 695–705.

Li, L., Xing, Y., Chang, D., Fang, S., Cui, B., Li, Q. et al. (2016) CaM/BAG5/Hsc70 signaling complex dynamically regulates leaf senescence. *Scientific Reports*, 6, 31889.

Liu, S., Wang, C., Liu, X., Navas-Castillo, J., Zang, L., Fan, Z. et al. (2021) Tomato chlorosis virus-encoded p22 suppresses auxin signalling to promote infection via interference with SKP1-Cullin-F-box(TIR1) complex assembly. *Plant, Cell & Environment*, 44, 3155–3172.

Martínez-Zubiaur, Y., Fiallo-Olivé, E., Carrillo-Tripp, J. & Rivera-Bustamante, R. (2008) First report of tomato chlorosis virus infecting tomato in single and mixed infections with tomato yellow leaf curl virus in Cuba. *Plant Disease*, 92, 836.

Mizushima, N. (2010) The role of the Atg1/ULK1 complex in autophagy regulation. *Current Opinion in Cell Biology*, 22, 132–139.

Mizushima, N., Levine, B., Cuervo, A.M. & Klionsky, D.J. (2008) Autophagy fights disease through cellular self-digestion. *Nature*, 451, 1069–1075.

Ng, S., De Clercq, I., Van Aken, O. et al. (2014) Anterograde and retrograde regulation of nuclear genes encoding mitochondrial proteins during growth, development, and stress. *Molecular Plant*, 7, 1075–1093.

Niu, E., Ye, C., Zhao, W., Kondo, H., Wu, Y., Chen, J. et al. (2022) Coat protein of Chinese wheat mosaic virus upregulates and interacts with cytosolic glyceraldehyde-3-phosphate dehydrogenase, a negative regulator of plant autophagy, to promote virus infection. *Journal of Integrative Plant Biology*, 64, 1631–1645.

Pallas, V. & García, J.A. (2011) How do plant viruses induce disease? Interactions and interference with host components. *The Journal of General Virology*, 92, 2691–2705.

Rothenburg, S. & Brennan, G. (2020) Species-specific host–virus interactions: implications for viral host range and virulence. *Trends in Microbiology*, 28, 46–56.

Shang, K., Xu, Y., Cao, W., Xie, X., Zhang, Y., Zhang, J. et al. (2022) Potato (*Solanum tuberosum* L.) non-specific lipid transfer protein StLTP6 promotes viral infection by inhibiting virus-induced RNA silencing. *Planta*, 256, 54.

Shukla, A., Hoffmann, G., Kushwaha, N.K., López-González, S., Hofius, D. & Hafrén, A. (2022) Salicylic acid and the viral virulence factor 2b regulate the divergent roles of autophagy during cucumber mosaic virus infection. *Autophagy*, 18, 1450–1462.

Suttangkakul, A., Li, F., Chung, T. & Vierstra, R.D. (2011) The ATG1/ATG13 protein kinase complex is both a regulator and a target of autophagic recycling in *Arabidopsis*. *The Plant Cell*, 23, 3761–3779.

Takayama, S., Sato, T., Krajewski, S., Kochel, K., Iriwe, S., Milian, J.A. et al. (1995) Cloning and functional analysis of BAG-1: a novel Bcl-2-binding protein with anti-cell death activity. *Cell*, 80, 279–284.

Teardo, E., Carraretto, L., Wagner, S., Formentin, E., Behera, S., de Bortoli, S. et al. (2017) Physiological characterization of a plant mitochondrial calcium uniporter in vitro and in vivo. *Plant Physiology*, 173, 1355–1370.

Van Aken, O. & Van Breusegem, F. (2015) Licensed to kill: mitochondria, chloroplasts, and cell death. *Trends in Plant Science*, 20, 754–766.

Wisler, G.C., Li, R.H., Liu, H.Y., Lowry, D.S. & Duffus, J.E. (1998) Tomato chlorosis virus: a new whitefly-transmitted, phloem-limited, bipartite closterovirus of tomato. *Phytopathology*, 88, 402–409.

Yang, M., Ismayil, A. & Liu, Y. (2020) Autophagy in plant–virus interactions. *Annual Review of Virology*, 7, 403–419.

Yang, M., Zhang, Y., Xie, X., Yue, N., Li, J., Wang, X.B. et al. (2018) Barley stripe mosaic virus γb protein subverts autophagy to promote viral infection by disrupting the ATG7-ATG8 interaction. *The Plant Cell*, 30, 1582–1595.

You, Q., Zhai, K., Yang, D., Yang, W., Wu, J., Liu, J. et al. (2016) An E3 ubiquitin ligase-BAG protein module controls plant innate immunity and broad-spectrum disease resistance. *Cell Host & Microbe*, 20, 758–769.

Zhou, S., Hong, Q., Li, Y., Li, Q. & Wang, M. (2018) Autophagy contributes to regulate the ROS levels and PCD progress in TMV-infected tomatoes. *Plant Science*, 269, 12–19.

SUPPORTING INFORMATION

Additional supporting information can be found online in the Supporting Information section at the end of this article.

How to cite this article: Shang, K., Xiao, L., Zhang, X., Zang, L., Zhao, D., Wang, C. et al. (2023) Tomato chlorosis virus p22 interacts with NbBAG5 to inhibit autophagy and regulate virus infection. *Molecular Plant Pathology*, 24, 425–435. Available from: https://doi.org/10.1111/mpp.13311